

Highly strained 1.24- μm InGaAs/GaAs quantum-well lasers

L. W. Sung^{a)} and H. H. Lin

*Department of Electrical Engineering and Graduate Institute of Electronics Engineering,
National Taiwan University, Taipei, Taiwan, Republic of China*

(Received 20 January 2003; accepted 23 June 2003)

Highly strained InGaAs/GaAs quantum wells grown at very low temperature (380 °C) have been studied. The critical thickness of the $\text{In}_{0.38}\text{Ga}_{0.62}\text{As}$ quantum well is 8.8 nm and the photoluminescence peak is at 1.24 μm . An edge-emitting $\text{In}_{0.388}\text{Ga}_{0.612}\text{As}/\text{GaAs}$ quantum-well laser demonstrates an emission wavelength of 1.244 μm at 18 °C. The threshold current density is 405 A/cm^2 for an as-cleaved diode laser with 873- μm cavity length. The internal quantum efficiency and laser cavity loss are 93% and 6.4 cm^{-1} , respectively. © 2003 American Institute of Physics. [DOI: 10.1063/1.1600504]

Highly strained InGaAs/GaAs quantum-well (QW) lasers operating beyond 1.2 μm are of considerable interest in high-speed data communications through standard single-mode fiber in metropolitan-area-network, wide-area-network,¹ and local-area-network applications.^{2–4} The high characteristic temperature T_0 , that comes from better electron confinement, and the availability of AlAs/GaAs distributed Bragg reflector that can be directly deposited in vertical-cavity surface-emitting laser fabrication make GaAs-based long-wavelength lasers outperform the currently used InP-based lasers.^{2,5,6} Many efforts have been devoted to this topic, including the InGaAsN/GaAs QW, GaAsSb/GaAs type-II QW, and In(Ga)As/GaAs quantum-dot material systems. All of these approaches have demonstrated their potential in long-wavelength GaAs-based lasers. However, because of the relative simple and mature techniques, the highly strained InGaAs/GaAs QW laser is still a promising candidate for laser applications whose operating wavelength is not far beyond 1.2 μm . Moreover, the proper growth control of highly strained InGaAs QW growth is also an important step in the optimization of InGaAsN QW lasers.^{5,7,8}

Due to the constraints of critical thickness and indium composition, the optical quality of InGaAs QWs degrade rapidly when its transition wavelength is over 1.1 μm .^{5,9} Great care must be taken with respect to the control of the growth conditions. Different approaches, such as the introduction of GaAsP strain-compensated barrier,^{2,10} and the use of Sb surfactant,³ have been applied to inhibit the relaxation of highly strained InGaAs QWs grown on GaAs substrate, and extended the transition wavelength to 1,200 ~ 1,225 nm.^{1–3,5–7,11}

In this letter, we demonstrate a highly strained InGaAs QW laser with low threshold current density grown by low-temperature-growth method. The emission wavelength of the laser is 1.244 μm .

The QW samples and laser structure were grown on *n*-type (001)-oriented GaAs substrates by using VG-V80H gas-source molecular-beam epitaxy system (GSMBE). Group-V sources were As_2 and P_2 beams cracked from AsH_3 and PH_3 . Group-III sources, Ga and In fluxes, were provided

by conventional K-cells. Si and Be were employed as *n*-type and *p*-type dopants. An IRCON pyrometer was used to probe the substrate temperature. Reflection high-energy electron diffraction (RHEED) was used to monitor the surface condition during the growth. After the epitaxial growth, double crystal x-ray diffraction was applied to verify the composition and thickness of epitaxial layers. Photoluminescence (PL) was performed to investigate the optical quality of epitaxial films at room temperature. The excitation source was a 514.5-nm Ar^+ laser and the luminescence was recorded with an InGaAs detector through a SPEX 500M spectrometer.

The samples designed to investigate the critical thickness consist of a GaAs buffer layer, a 200-nm-thick InGaP cladding layer, a 120-nm-thick GaAs layer, a highly strained $\text{In}_{0.38}\text{Ga}_{0.62}\text{As}$ QW with the well thickness ranging from 6.8 to 12.1 nm, a 120-nm-thick GaAs layer, and a 200-nm-thick InGaP cladding layer. The highly strained QW layer was grown at 380 °C so as to suppress strain relaxation, and the rest layers were deposited at 440 °C. In the low-temperature epitaxial growth, the V/III-ratio control had been considered as an important growth parameter in literature¹² and in our preliminary experimental results. It was kept < 1.2 in the growth of samples discussed in this letter to minimize the defects induced by the low growth temperature. Throughout the epitaxial growth of the highly strained QW, RHEED revealed a 1×1 streaky pattern. No spotty pattern was observed. It illustrates the flat growth surface during the epitaxial growth of the highly strained layers. Critical thickness of the $\text{In}_{0.38}\text{Ga}_{0.62}\text{As}$ QW was determined from the decline in the optical quality of the QW samples.¹³ The PL integrated intensity and peak transition wavelength of these samples are shown in Fig. 1. QW samples with well widths thinner than 8.8 nm show no significant difference in optical quality. As the well width is further increased, the PL intensity degrades steadily, due to the relaxation of the strained layer. Critical thickness of $\text{In}_{0.38}\text{Ga}_{0.62}\text{As}$ layer on GaAs substrate is determined to be 8.8 nm at this growth condition, and the corresponding transition wavelength is around 1.24 μm . The critical thickness result of $\text{In}_{0.38}\text{Ga}_{0.62}\text{As}/\text{GaAs}$ QW exceeds the value predicted by the Matthews and Blakeslee model ($\sim 6.5 \text{ nm}$).¹³ The experimental result shows that the forma-

^{a)}Electronic mail: sam@epicenter.ee.ntu.edu.tw

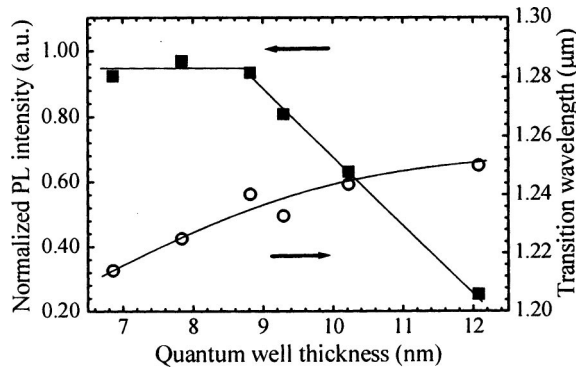


FIG. 1. PL integrated intensity and peak wavelength versus well thickness plots of $\text{In}_{0.38}\text{Ga}_{0.62}\text{As}/\text{GaAs}$ QW PL samples.

tion of misfit dislocations was suppressed by low-temperature-growth method effectively. The irregular variation of transition wavelength around 9-nm well width in Fig. 1 is attributed to the run-to-run fluctuation of the indium flux.

A separate-confinement heterostructure $\text{InGaAs}/\text{GaAs}$ laser was designed and grown with the low-temperature-growth method. The laser structure is shown in Table I. Single InGaAs QW is placed in the center of the GaAs waveguide layer. The n -side cladding InGaP layer is Si-doped, with a carrier density of $1 \times 10^{18} \text{ cm}^{-3}$. In order to reduce the free carrier absorption, the carrier density of the Be-doped InGaP cladding layer is graded from 1×10^{17} to $1 \times 10^{18} \text{ cm}^{-3}$. Finally, a $0.3\text{-}\mu\text{m}$ -thick p^+ - GaAs layer is heavily doped to $1 \times 10^{19} \text{ cm}^{-3}$ to minimize the contact resistance. The highly strained QW of the laser was grown using the same growth conditions of the PL samples as described previously. This kind of Al-free laser structure had shown its superior property in device reliability.¹⁴ The grown laser sample was then processed into $50\text{-}\mu\text{m}$ -wide broad-area lasers by standard photolithography and wet etching methods. Uncoated lasers were tested under pulse operation with a $4\text{-}\mu\text{s}$ pulse width and 500-Hz repetition rate. A calibrated Newport-818IR Ge detector was used to measure the emission power. And the spectra of lasers were recorded by using an HP70951A optical spectrum analyzer. Figure 2 shows the emission spectrum of a diode laser with $873\text{-}\mu\text{m}$ cavity. The laser was operated at 18°C with an injection current of $1.02 I_{\text{th}}$. As can be seen, the emission wavelength is at $1.244 \mu\text{m}$.

From the external quantum efficiency versus cavity length plot, internal quantum efficiency and the internal losses can be determined. The results are shown in Fig. 3. The extracted internal quantum efficiency is 93%, and the internal loss is 6.4 cm^{-1} . The loss is slightly higher than the

TABLE I. $\text{InGaAs}/\text{GaAs}$ single-QW laser layer structure.

Layer	Composition	Thickness	Doping
Contact	p^+ GaAs	$0.3 \mu\text{m}$	$>1 \times 10^{19}/\text{cm}^3$
Cladding	p InGaP	$1.7 \mu\text{m}$	$1 \times 10^{17}/\text{cm}^3$ $1 \times 10^{18}/\text{cm}^3$
Barrier	GaAs	120 nm	...
Well	$\text{In}_{0.38}\text{Ga}_{0.62}\text{As}$	8.8 nm	...
Barrier	GaAs	120 nm	...
Cladding	n InGaP	$1.7 \mu\text{m}$	$1 \times 10^{18}/\text{cm}^3$
Substrate	n^+ GaAs		

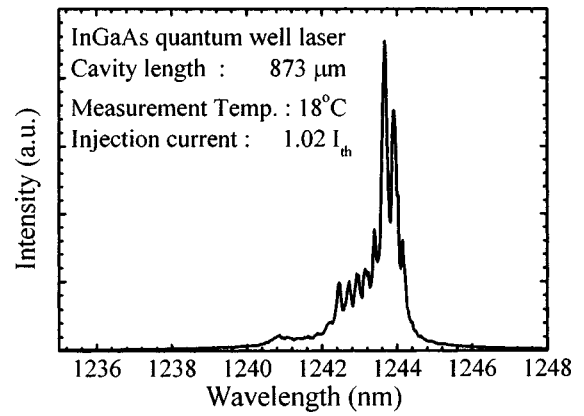


FIG. 2. Room-temperature spectrum of $\text{InGaAs}/\text{GaAs}$ QW laser with $873\text{-}\mu\text{m}$ -long cavity.

typical value of $\text{InGaAs}/\text{GaAs}$ lasers, which is due to the defects induced by low growth temperature in GaAs waveguide layer. The inset in Fig. 3 shows the threshold current densities of InGaAs lasers as a function of reciprocal cavity length. The threshold current density of the laser with $873\text{-}\mu\text{m}$ cavity is 405 A/cm^2 , and the fitted threshold current density at infinite cavity length is 274 A/cm^2 for this highly-strained QW laser. Figure 4 shows the threshold current density of the highly strained InGaAs lasers as a function of emission wavelength. Besides this work, other reported values are also included in the figure. With proper control of V/III ratio at the growth, the active layer was grown at very low temperature without introducing a large amount of defect. As can be seen, our laser emitting at 1244 nm is achieved with only a slight increase in threshold current density.

Figure 5 shows the temperature variation of the threshold current density I_{th} and the differential quantum efficiency η_d of the laser with $873\text{-}\mu\text{m}$ -long cavity. The characteristic temperatures of laser are determined by using the following formulas:

$$\frac{1}{T_0} = \frac{1}{I_{\text{th}}} \frac{dI_{\text{th}}}{dT}, \quad (1)$$

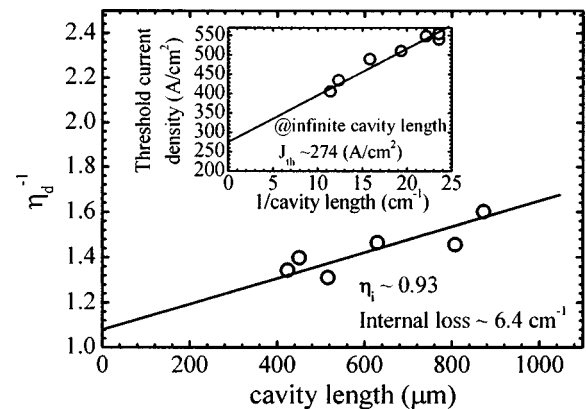


FIG. 3. Inverse external quantum efficiency of broad-area lasers as a function of cavity length. The internal quantum efficiency and loss can be fitted from this plot. Inset shows the threshold current density versus reciprocal cavity length plot. The fitted threshold current density for infinite cavity length is 274 A/cm^2 .

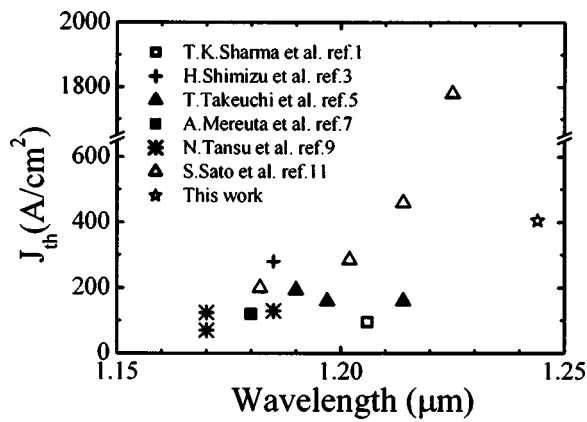


FIG. 4. Threshold current density of the highly strained InGaAs QW lasers as a function of emission wavelength. Besides this work, the other reported values are also included.

$$\frac{1}{T_1} = \frac{1}{\eta_d} \frac{d\eta_d}{dT}, \quad (2)$$

where T is the operating temperature. The characteristic temperatures T_0 and T_1 of this highly strained QW laser are 150 and 598 K in the temperature range from 18 to 89 °C, respectively. At 89 °C, the laser has its wavelength shifted to

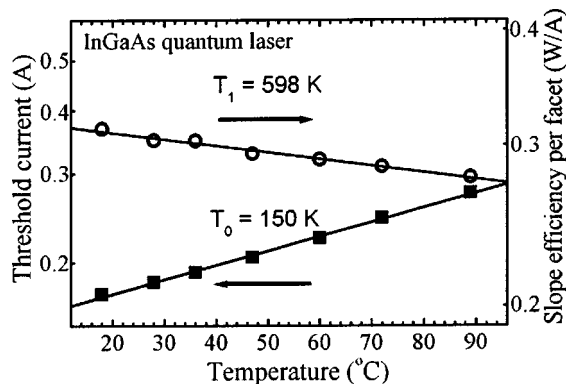


FIG. 5. Temperature characteristics of highly strained InGaAs/GaAs laser with 873- μ m-long cavity.

1.276 μ m and shows a single-facet slope efficiency of 0.28 W/A. The temperature characteristics are comparable to those of the high-quality InGaAs/InGaP/GaAs QW lasers operated at shorter wavelength, about two times higher than the currently used InGaAsP/InP lasers operated at similar wavelength. The superior temperature characteristics and optical quality makes the InGaAs QW laser a suitable candidate for fiber-communication applications under heat-sink-free operation.

In conclusion, we investigated the critical thickness of the In_{0.38}Ga_{0.62}As layer grown by GSMBE. By using low-temperature-growth method, formation of misfit dislocations was suppressed effectively in the growth of the 8.8-nm-thick highly strained InGaAs layer. A low threshold current density InGaAs/GaAs QW laser with 1.244- μ m emission wavelength is demonstrated.

This work was supported by the National Science Council and the Ministry of Education of the ROC under Contract Nos. NSC 90-2215-E-002-030 and 89-N-FA01-2-4-3, respectively.

- ¹T. K. Sharma, M. Zorn, F. Bugge, R. Hülsewede, G. Erbert, and M. Weyers, *IEEE Photonics Technol. Lett.* **14**, 887 (2002).
- ²S. W. Ryu and P. D. Dapkus, *Electron. Lett.* **37**, 177 (2001).
- ³H. Shimizu, K. Kumada, S. Uchiyama, and A. Kasukawa, *Electron. Lett.* **36**, 1379 (2000).
- ⁴T. Kondo, D. Schlenker, T. Miyamoto, Z. Chen, M. Kawaguchi, E. Gouardes, F. Koyama, and K. Iga, *Jpn. J. Appl. Phys.* **40**, 467 (2002).
- ⁵T. Takeuchi, Y. L. Chang, A. Tandon, D. Bour, S. Corzine, R. Twist, M. Tan, and H. C. Luan, *Appl. Phys. Lett.* **80**, 2445 (2002).
- ⁶F. Salomonsson, C. Asplund, P. Sundgren, G. Plaine, S. Mogg, and M. Hammer, *Electron. Lett.* **37**, 957 (2001).
- ⁷A. Mereuta, S. Bouchoule, F. Alexandre, I. Sagnes, J. Decobert, and A. Ougazzaden, *Electron. Lett.* **36**, 436 (2000).
- ⁸N. Tansu and L. J. Mawst, *IEEE Photonics Technol. Lett.* **14**, 444 (2002).
- ⁹N. Tansu, Y. L. Chang, T. Takeuchi, D. P. Bour, S. W. Corzine, M. R. T. Tan, and L. J. Mawst, *IEEE J. Quantum Electron.* **38**, 640 (2002).
- ¹⁰N. Tansu and L. J. Mawst, *IEEE Photonics Technol. Lett.* **13**, 179 (2001).
- ¹¹S. Sato and S. Satoh, *IEEE J. Sel. Top. Quantum Electron.* **5**, 707 (1999).
- ¹²T. Kitada, K. Nii, T. Hiraoka, S. Shimomura, and S. Hiyamizu, *J. Vac. Sci. Technol. B* **19**, 1546 (2001).
- ¹³D. Schlenker, T. Miyamoto, Z. Chen, F. Koyama, and K. Iga, *J. Cryst. Growth* **209**, 27 (2000).
- ¹⁴L. J. Mawst, A. Bhattacharya, J. Lopez, D. Botez, D. Z. Garbuzov, L. Demarco, J. C. Connolly, M. Jansen, F. Fang, and R. F. Nabiev, *Appl. Phys. Lett.* **69**, 1532 (1996).

Applied Physics Letters is copyrighted by the American Institute of Physics (AIP). Redistribution of journal material is subject to the AIP online journal license and/or AIP copyright. For more information, see <http://ojps.aip.org/aplo/aplcr.jsp>
Copyright of Applied Physics Letters is the property of American Institute of Physics and its content may not be copied or emailed to multiple sites or posted to a listserv without the copyright holder's express written permission. However, users may print, download, or email articles for individual use.